POLARIZATION CATASTROPHE AND SUPERCRITICAL IMPURITIES IN GRAPHENE

Leonid Levitov (MIT)

collaboration:

Andrey Shytov, Michael Katsnelson, Dima Abanin, Patrick A Lee

A. I. Larkin memorial conference, Chernogolovka

June 25, 2007

Graphene background,
Quantum Hall effect,
edge states,
p-n junctions

Transport in graphene

New 2d electron system:
1) Nano; 2) Tunable; 3) New physics (e & h, QHE)

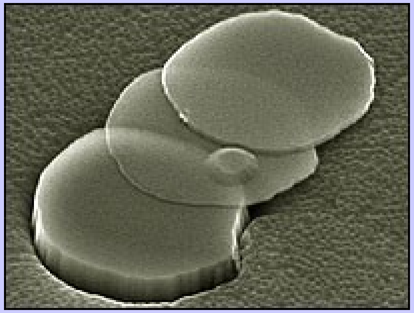

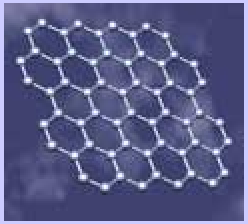

Monolayer graphene, Carbon lattice

Massless Dirac electrons, d=2

Field effect enabled by gating:
mobility, density vs gate voltage

Band structure, Dirac points

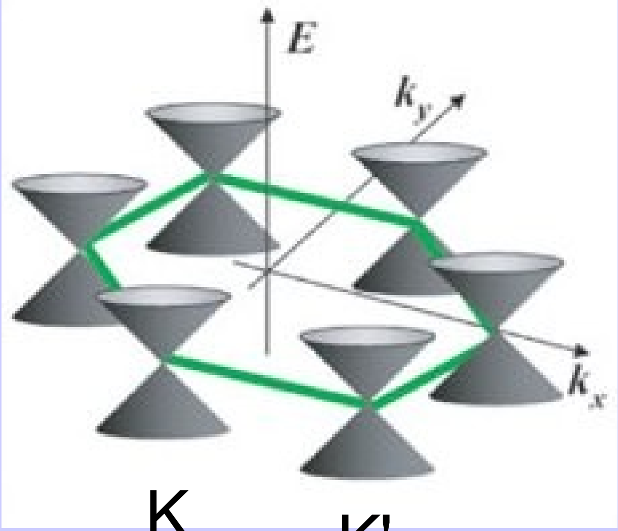

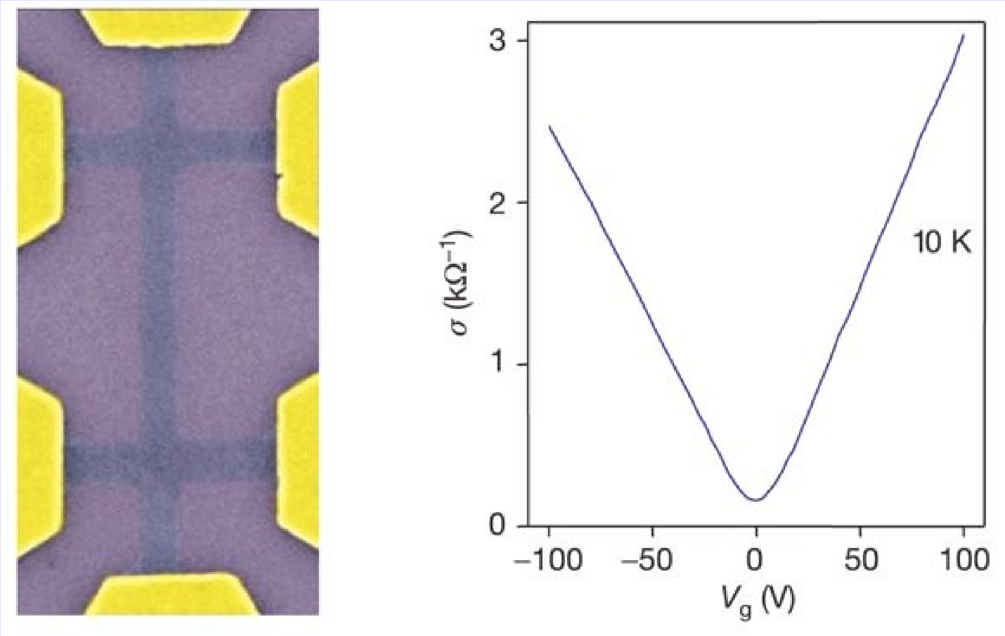

Novoselov et al, 2004, Zhang et al, 2005

"Half-integer" Quantum Hall Effect

Single-layer graphene:
QHE plateaus observed at

$$\nu = 4 \times (0, \pm 1/2, \pm 3/2 \ldots)$$

4=2x2 spin and valley degeneracy

double-layer: one layer:

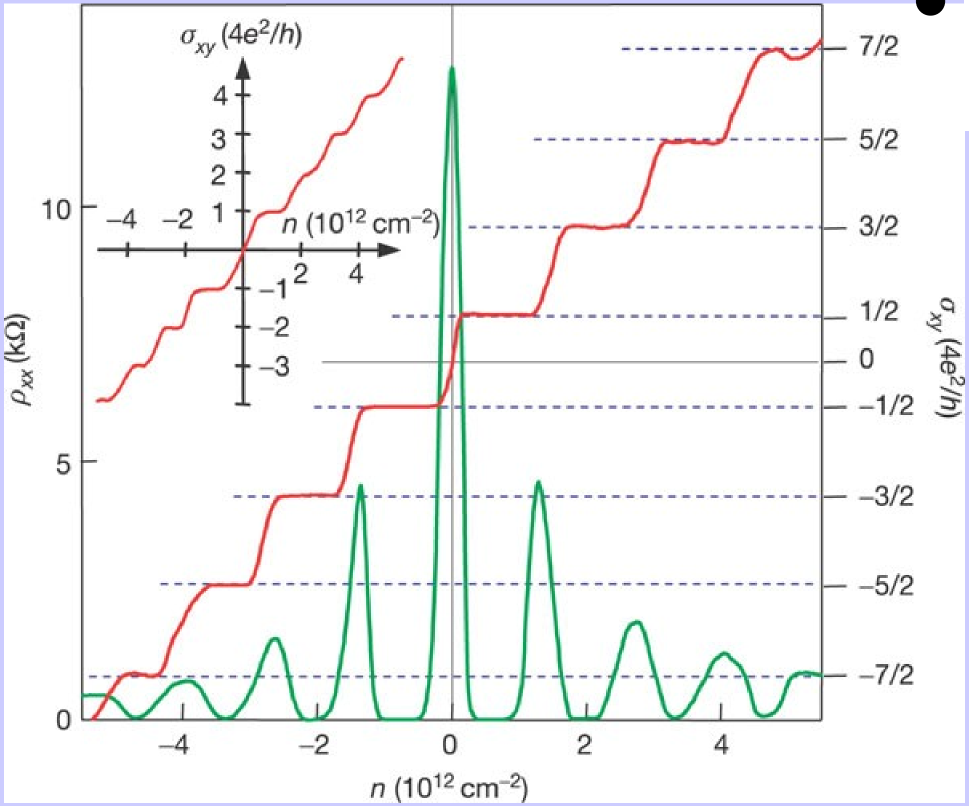

Landau level spectrum

$$E_n = \mathrm{sgn}(n)|n|^{1/2}\epsilon_0, \quad \epsilon_0 = \hbar v_0 \left(2eB/\hbar c\right)^{1/2}$$

- Particle-hole symmetric; has a *zero mode*
- $E_n \propto \sqrt{n}, \sqrt{B}$
- Separation between low-lying LL is very large, 1000 K at $B = 10\,\mathrm{T} \longrightarrow$ *room temperature QHE*

Recently: QHE at T=300K

Explanations of half-integer QHE:
(i) anomaly of Dirac fermions;
(ii) Berry phase;
(iii) counter-propagating edge states

Novoselov et al, 2005, Zhang et al, 2005

Chiral edge states

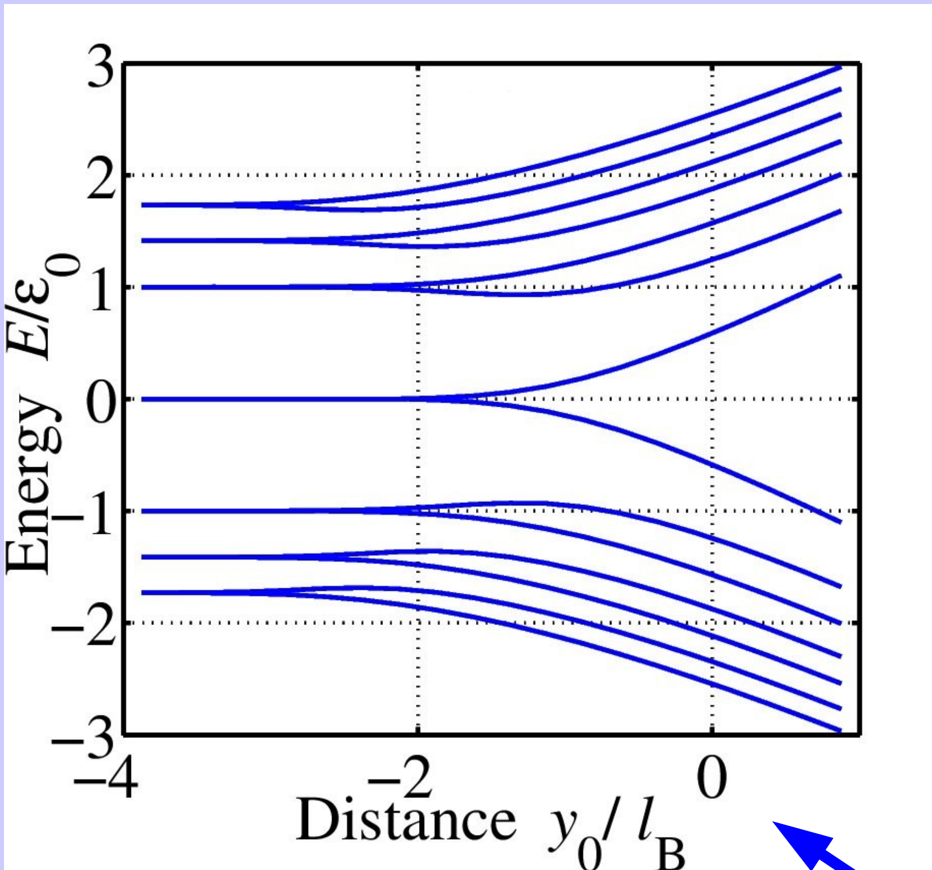

Edge states properties:

- KK' splitting due to mixing at the boundary;
- Counter-propagating electron and hole states;
- Symmetric splitting of n=0 LL
- Universality, same for other edge types;
- The odd numbers of edge modes result in half-integer QHE

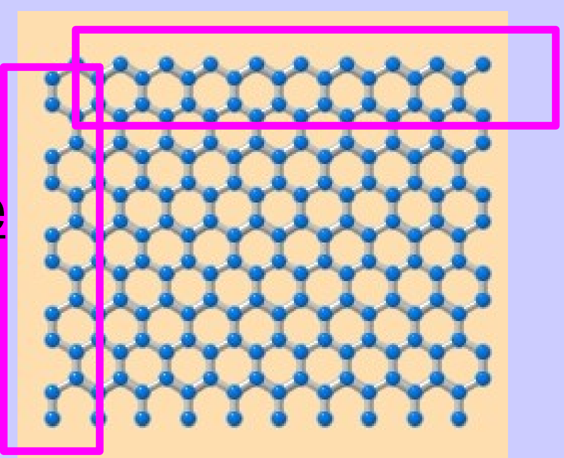

Edge states from 2d Dirac model

Abanin, Lee, LL, PRL 96, 176803 (2006)

Also: Peres, Guinea, Castro-Neto, 2005, Brey and Fertig, 2006

Graphene devices

Devices in patterned graphene:
- quantum dots (Manchester),
- nanoribbons (IBM, Columbia);

Local density control (gating):
- p-n and p-n-p junctions

(Stanford, Harvard, Columbia)

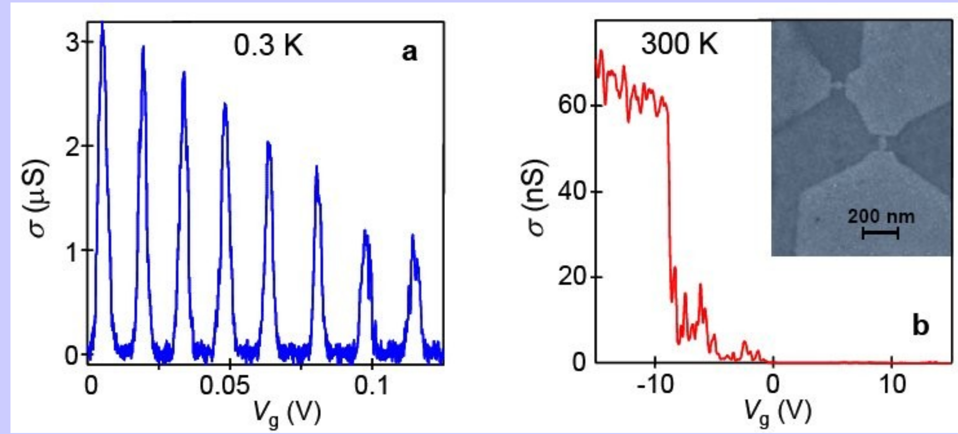

QHE in p-n junctions, integer and fractional quantization:

(i) g=2,6,10..., unipolar regime, (ii) g=1,3/2..., bipolar regime

B>0

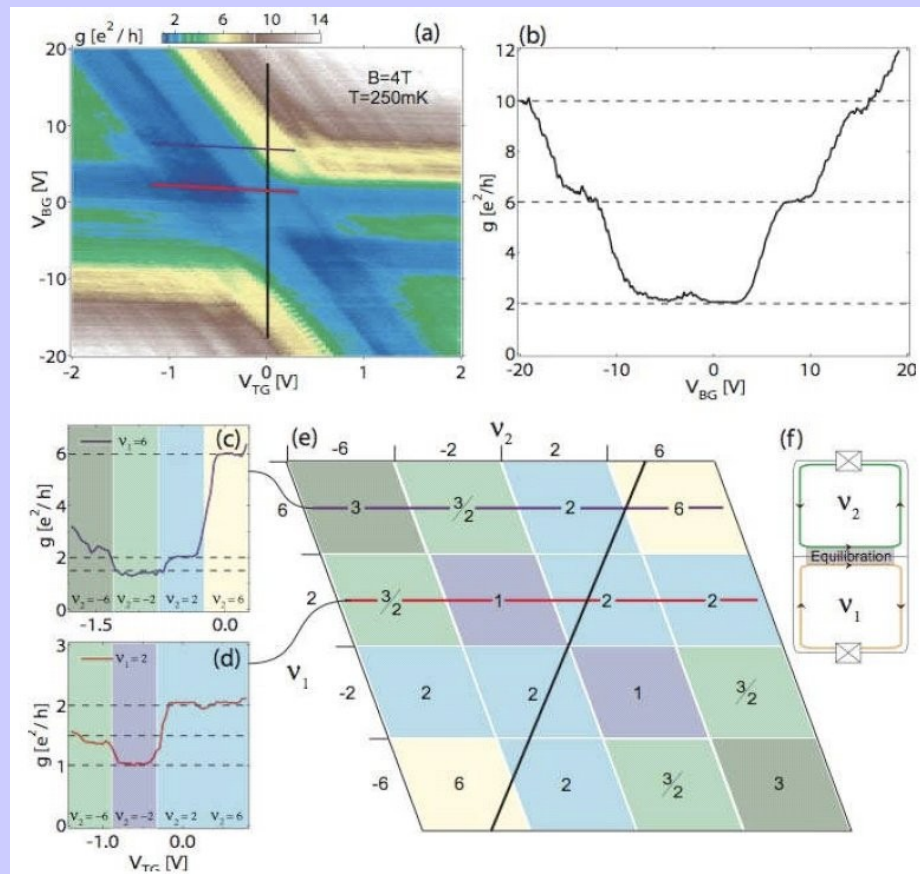

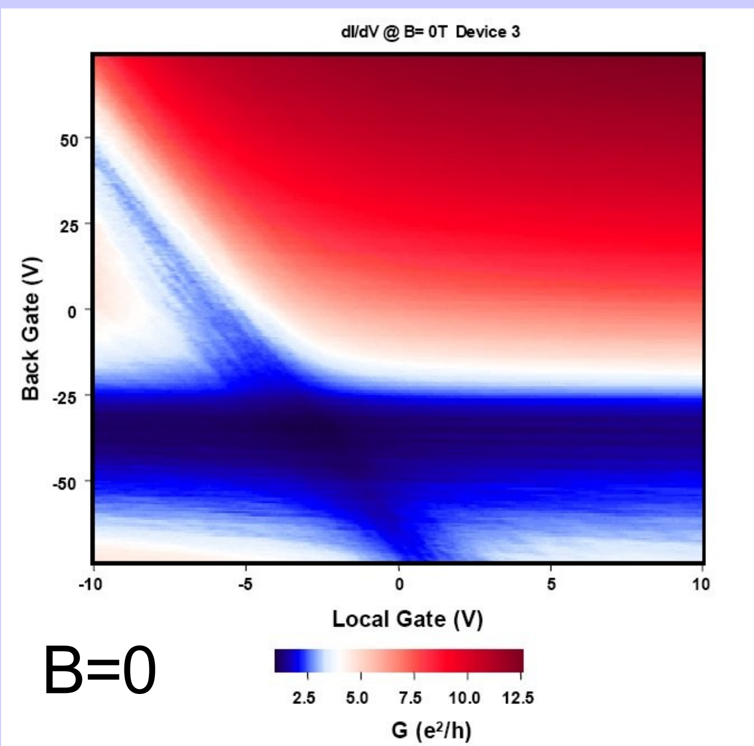

QHE in p-n junctions

p-n n-n, p-p

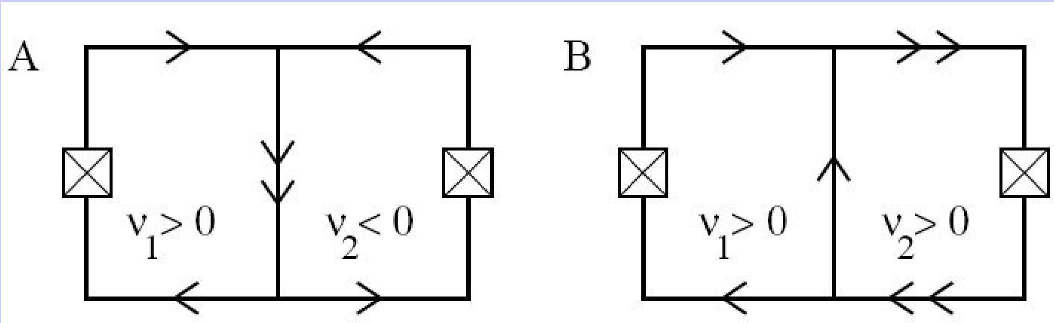

No mixing

$$g_{\rm nn} = g_{\rm pp} = \min(|\nu_1|, |\nu_2|) = 2, 6, 10\ldots$$

Noiseless transport

Mode mixing, but UCF suppressed

$$g_{\rm pn} = \frac{|\nu_1||\nu_2|}{|\nu_1| + |\nu_2|} = 1,\ \frac{3}{2},\ 3,\ \frac{5}{3}\ldots$$

Current partition, noise

Quantized conductance

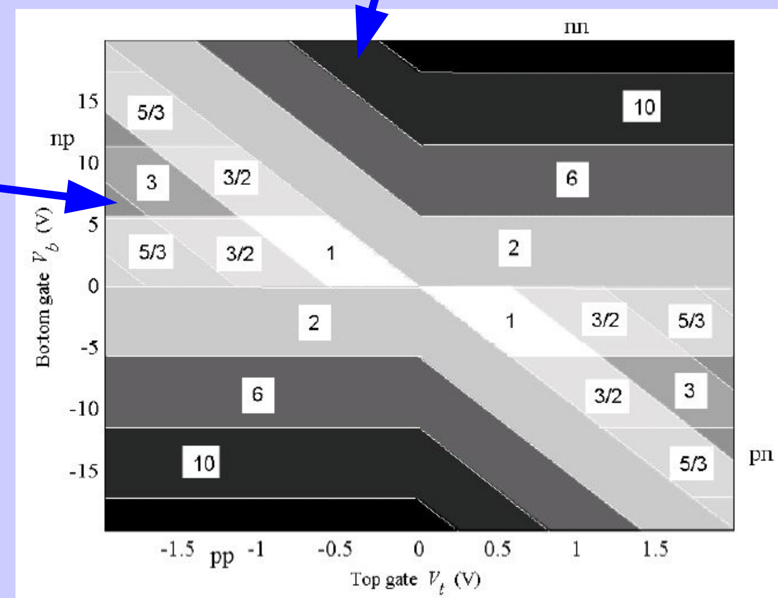

F>0

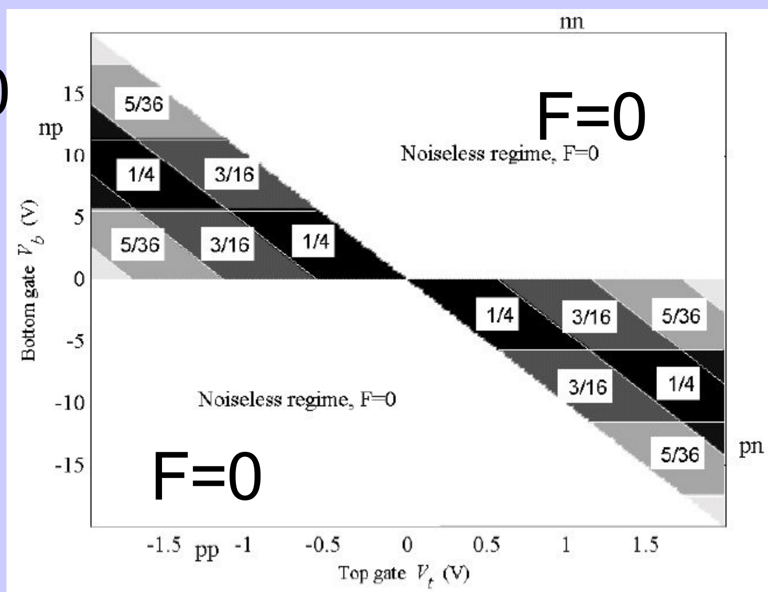

F>0

Quantized shot noise (fractional F=S/I)

Abanin & LL, Science 28 June 2007

Charge impurities in graphene, scattering, Dirac-Kepler, vacuum polarization, screening

Shytov, Katsnelson, LL (2007)

Transport theory

Facts:

- linear dependence of conductivity vs. electron density;
- minimal conductivity 4e^2/h

Born approximation:

$$\sigma = \frac{e^2}{\hbar} 2 k_F \ell = \frac{e^2}{\hbar} 2 E_F \tau_0 / \hbar, \quad \hbar/\tau_0 = 2\pi\nu_F \bar{V}^2$$

Charge impurities: dominant scattering mechanism (MacDonald, Ando)

$$V(q) = \frac{2\pi e^2}{\kappa(q + 4\alpha k_F)} \approx \frac{\hbar v \pi}{2k_F}, \quad \alpha = e^2/\kappa\hbar v \approx 2.5$$

$$\sigma \propto (4e^2/h) n_{el}/n_{imp}$$

Screening of impurity potential: no difference on the RPA level

Effects outside Born and RPA approximation?

Anomaly in Dirac theory of heavy atoms, Z>137

Textbook solution for hydrogenic spectrum fails at Z>137:

$$E_{n,j} = mc^2 \left[1 + \frac{(Z\alpha)^2}{\left(n - |\kappa| + \sqrt{\kappa^2 - (Z\alpha)^2}\right)^2} \right]^{-1/2}, \quad \alpha \equiv \frac{e^2}{\hbar c} = \frac{1}{137}, \quad n, \kappa = 1, 2, 3\ldots$$

Finite nuclear radius important at Z>137 (Pomeranchuk, Smorodinsky)

New spectrum at 137<Z<170;
Level diving one by one into the Dirac-Fermi sea at Z>170
(Zeldovich, Popov, Migdal)

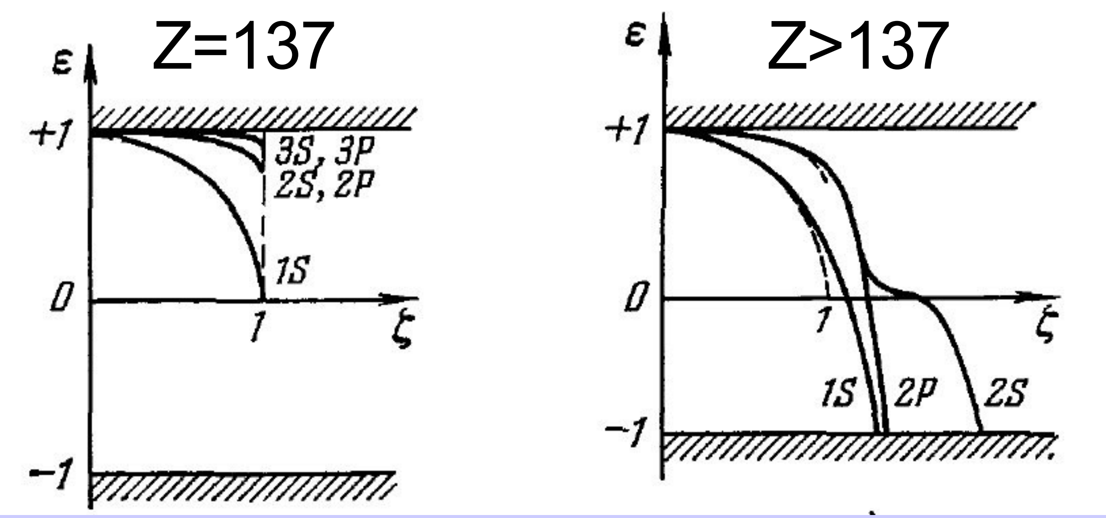

Quasiclassical interpretation:
collapsing trajectories in relativistic Kepler problem at $M < Ze^2/c$

Manifestation for massless Dirac particles: vacuum polarization

Critical Coulomb potentials in d=2:

$$\beta = \beta_c = \frac{1}{2}, \quad \beta \equiv \frac{Ze^2}{\kappa \hbar v_F}$$

$$Z_c \approx 1$$

In graphene:

$$\frac{e^2}{\hbar v_F} \approx 2.5$$

$$\kappa_{\mathrm{RPA}} \approx 5.$$

Easier to realize than Z>137 for heavy atoms!

Polarization charge localized on a lattice scale at $\beta < \frac{1}{2}$

Sachdev et al (CFT), Mirlin et al (RPA)

A power law for overcritical potential:

$$n_{\mathrm{pol}}(\rho) \approx -\frac{N\gamma\,\mathrm{sign}\,\beta}{2\pi^2\rho^2} + q_0\delta(\rho), \quad \gamma \equiv \sqrt{\beta^2 - \frac{1}{4}}$$

$$\frac{1}{2} < \beta < \frac{3}{2}$$

Friedel sum rule argument

Use scattering phase to evaluate polarization?

Caution: energy and radius dependence for Coulomb scattering

$$\beta < \beta_c : \quad \theta(k) \approx \beta \ln k\rho$$

$$\beta > \beta_c : \quad \theta(k) \approx \beta \ln k\rho - \gamma \text{sign}\, \beta \ln k r_0$$

Geometric part, not related to scattering, (deformed plane wave)

The essential part

$$Q_{\text{pol}}(\rho) = -N \frac{\theta(k \sim 1/\rho)}{\pi} = -\,\text{sign}\, \beta \frac{\gamma N}{\pi} \ln \frac{\rho}{2r_0}.$$

RG for polarization cloud

Log-divergence of polarization, negative sign,
but no overscreening!

RG flow of the net charge (source+polarization):

$$\frac{d\beta(\rho)}{d\ln\rho} = -\frac{N\,\mathrm{sign}\,\beta}{\pi\kappa}\gamma(\rho), \quad \beta > \beta_c$$

Polarization cloud radius:

$$\rho_* = r_0 \exp\left(\frac{\pi\kappa}{N}\cosh^{-1}(2\beta)\right)$$

Nonlinear screening of the charge in excess of 1/2

Oscillations in the local density of states

Standing wave in LDOS within polarization cloud

for overcritical Coulomb potential

period = 1/energy

period > lattice constant, can be probed with STM

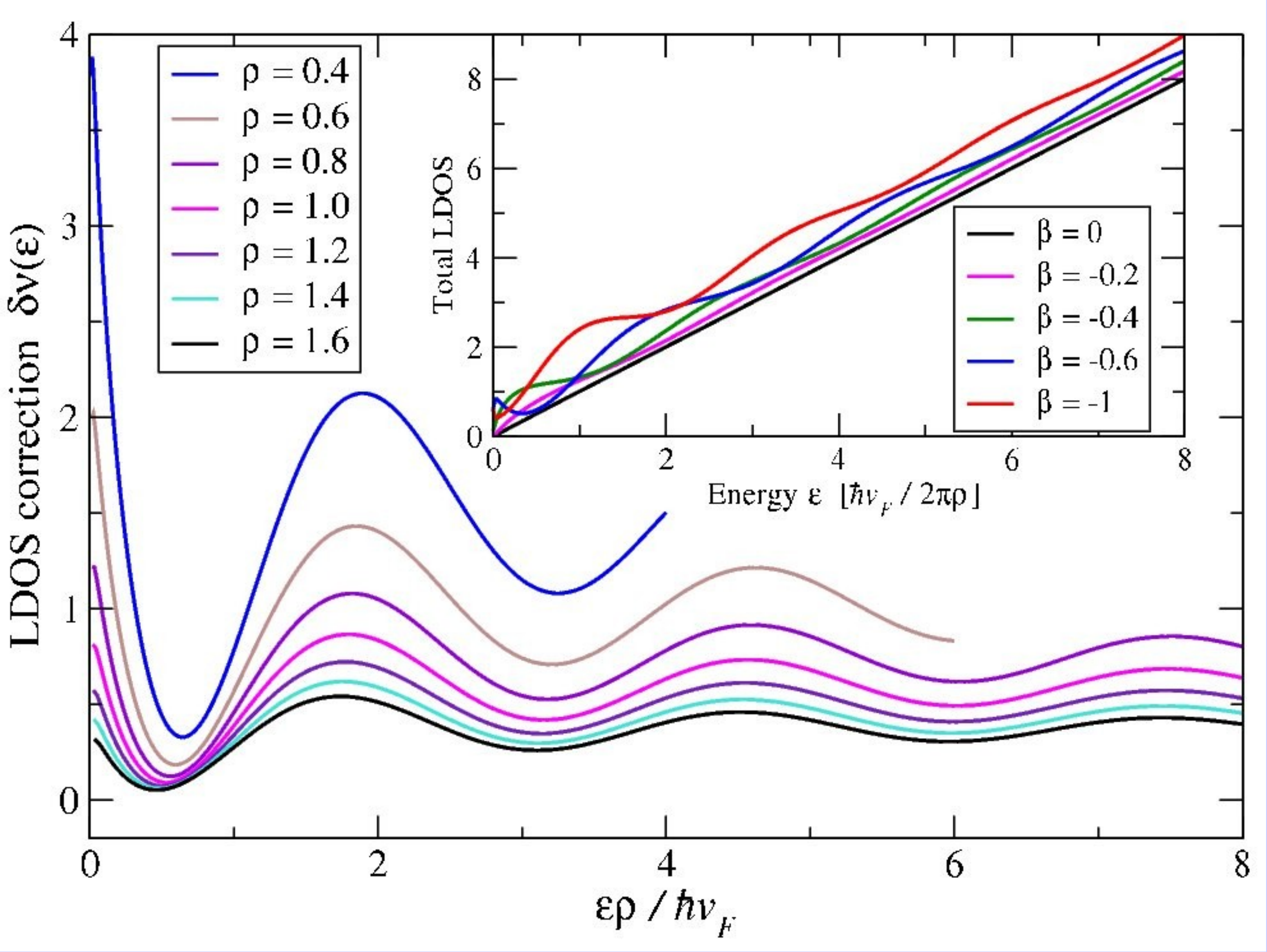

Summary

- No polarization away from impurity for charge below critical (in agreement with RPA)
- Power law 1/r^2 for polarization around an overcritical charge
- Log-divergence of the screening charge: nonlinear screening of the excess charge Q-1/2, spatial structure described by RG
- Long-period standing wave oscillations in LDOS around supercritical impurities

The End

Part II: Spin transport at graphene edge; Dissipative Quantum Hall effect

Abanin, Lee, LL, PRL 96, 176803 (2006)
Abanin, Novoselov, Zeitler, Lee, Geim, LL, cond-mat/0702125

Spin-polarized edge states for Zeeman-split Landau levels

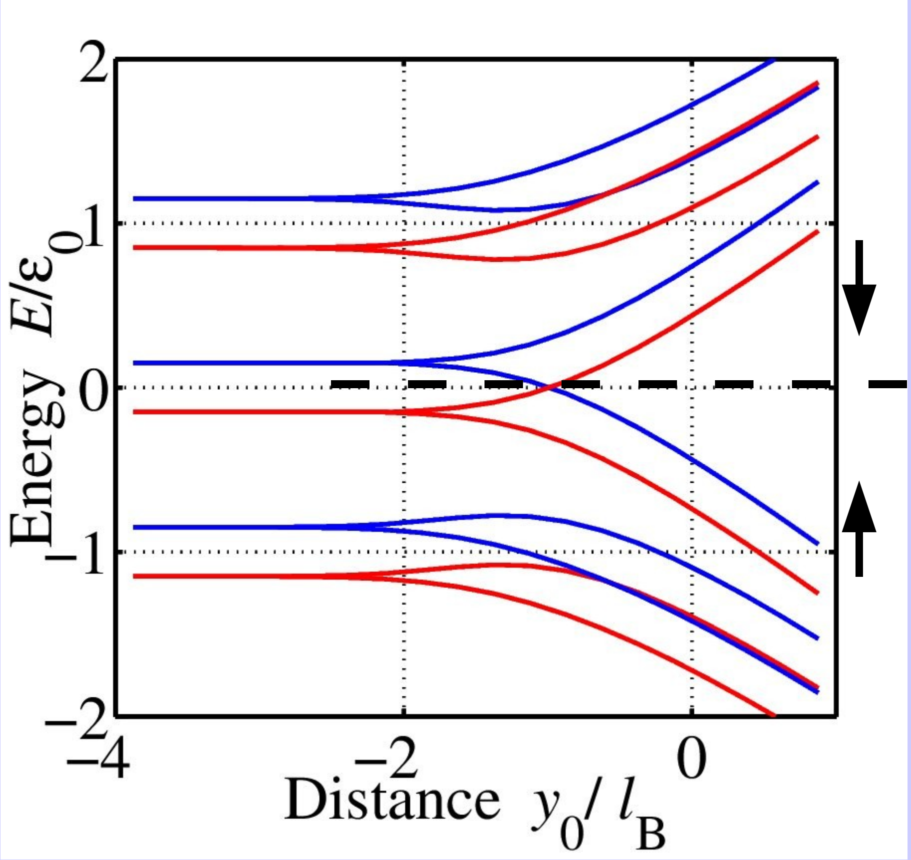

Near $\nu=0$, E=0:
(i) Two chiral counter-propagating edge states;
(ii) Opposite spin polarizations;
(iii) No charge current, but finite spin current.

Quantized spin Hall effect (charge Hall vanishes)

Edge transport as spin filter

Applications for spintronics

Similar to QSHE predicted by Kane and Mele (2005) in graphene with spin-orbital interaction (B=0, weak SO gap). Here a large gap!

What symmetry protects gapless edge states?

Gapless states, e.g. spin-split   Gapped states, e.g. valley-split

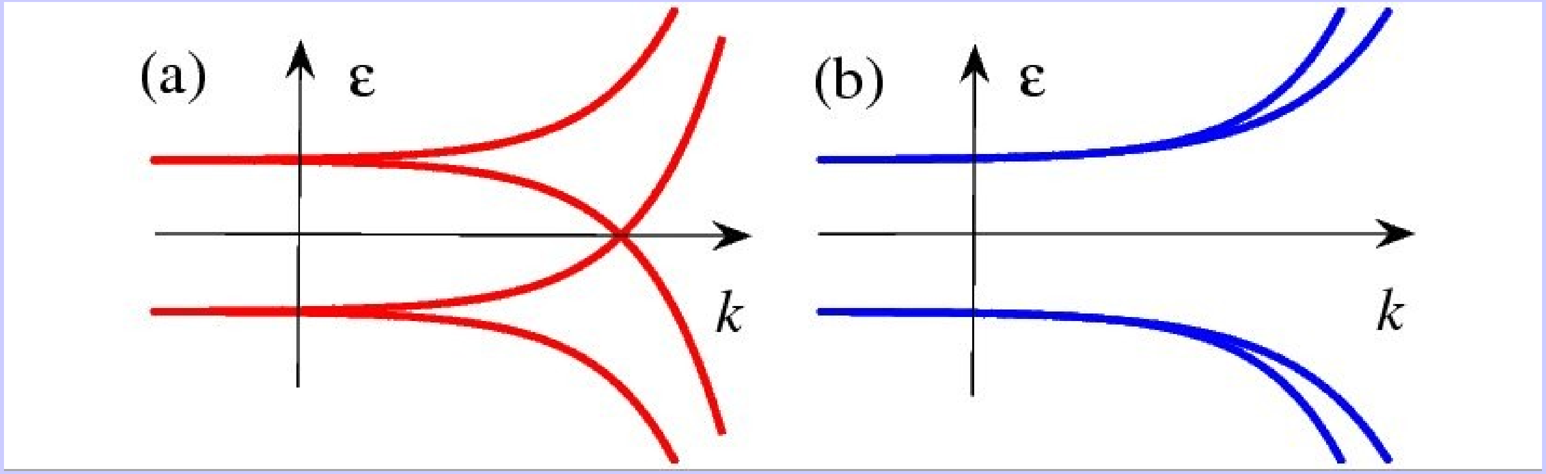

Special Z_2 symmetry requirements (Fu, Kane, Mele, 2006):
in our case, the Z_2 invariant is S_z which commutes with H

Resembles massless Dirac excitations in band-inverted heterojunctions, such as PbTe, protected by <u>supersymmetry</u> (Volkov and Pankratov, 1985)

Manifestations in transport near the neutrality point

Gapless spin-polarized states:

a) Longitudinal transport of 1d character;
b) Conductance of order unity, e^2/h,
at weak backscattering (SO-induced spin flips);
c) No Hall effect at $\nu=0$

Gapped states:

a) Transport dominated by bulk resistivity;
b) Gap-activated temperature dependent resistivity;
c) Hopping transport, insulator-like T-dependence
d) Zero Hall plateau

Dissipative QHE near ν=0

Longitudinal and Hall resistance, T=4K, B=30T

Features:

a) Peak in ρxx with metallic T-dependence;

b) Resistance at peak ~h/e^2

c) Smooth sign-changing ρxy no plateau;

d) Quasi-plateau in calculated Hall conductivity, double peak in longitudinal conductivity

Novoselov, Geim et al, 2006

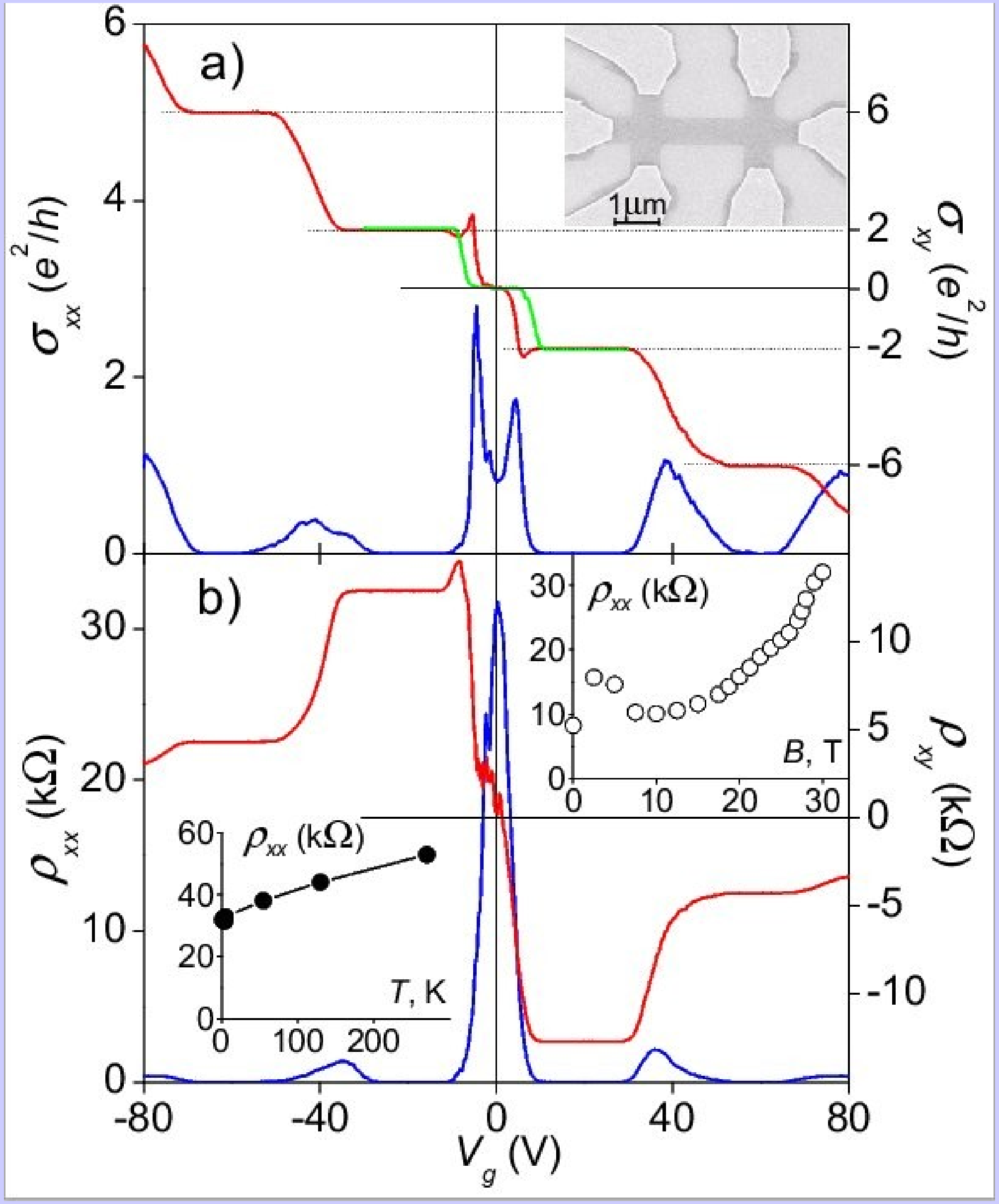

Edge transport model

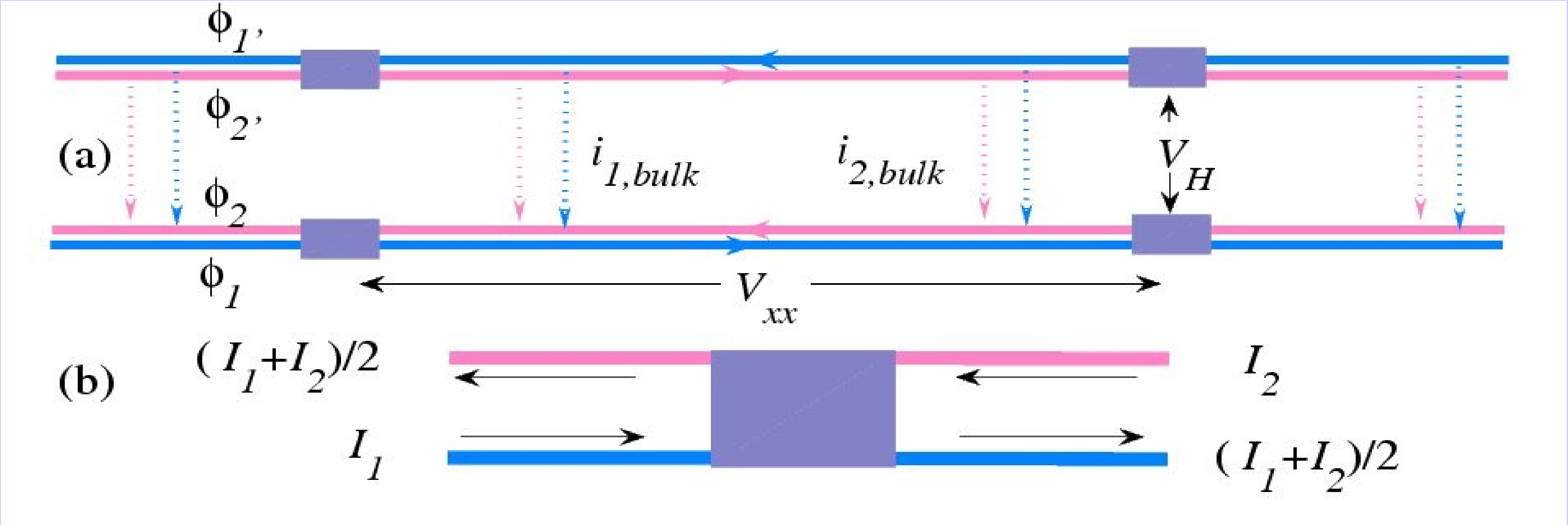

$$I_1 = \frac{e^2}{h}\varphi_1, \quad I_2 = \frac{e^2}{h}\varphi_2, \quad I = I_1 - I_2$$

$$I_{1,2}^{(\mathrm{out})} = \frac{1}{2}(I_1 + I_2)$$

$$V_{\mathrm{probe}} = \frac{h}{e^2} I_{1,2}^{(\mathrm{out})}$$

Ideal edge states, contacts with full spin mixing:
voltage drop along the edge across each contact
universal resistance value

$$\Delta\varphi = \frac{h}{2e^2}(I_1 - I_2)$$

Dissipative edge, unlike conventional QHE!

Backscattering (spin-flips), nonuniversal resistance
Estimate mean free path ~0.5 μm

$$R_{xx} = (\gamma L + 1)\frac{h}{2e^2}$$

Transport coefficients versus filling factor

Broadened, spin-split Landau levels

Bulk conductivity short-circuits edge:

a) peak in ρ_{xx} at $\nu=0$;

b) smooth ρ_{xy}, sign change, no plateau

c) quasi-plateau in $G_{xy}=\rho_{xy}/(\rho_{xy}^2+\rho_{xx}^2)$;

d) double peak in $G_{xx}=\rho_{xx}/(\rho_{xy}^2+\rho_{xx}^2)$

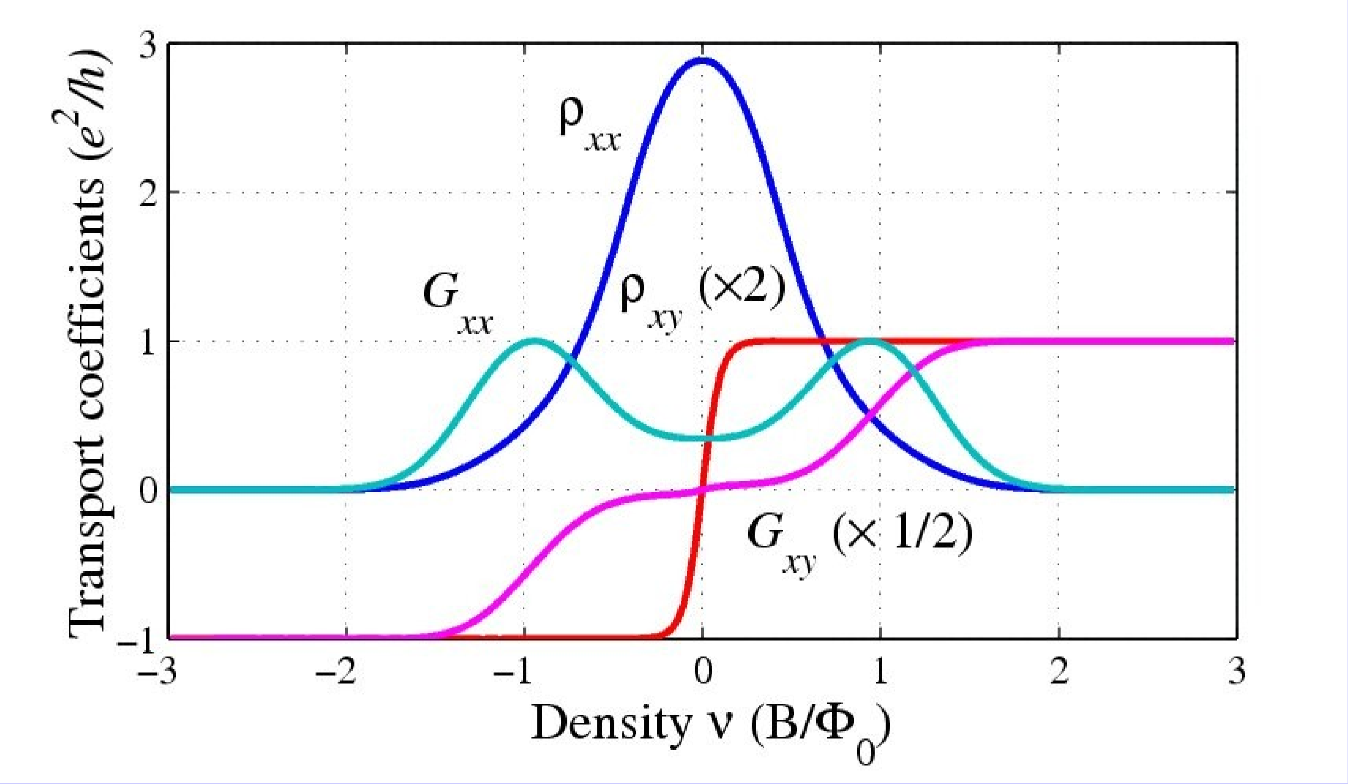

Model explains all general features of the data near $\nu=0$

The roles of bulk and edge transport interchange (cf. usual QHE): longitudinal resistivity due to edge transport, Hall resistivity due to bulk.

Spintronics in grapene: chiral spin edge transport

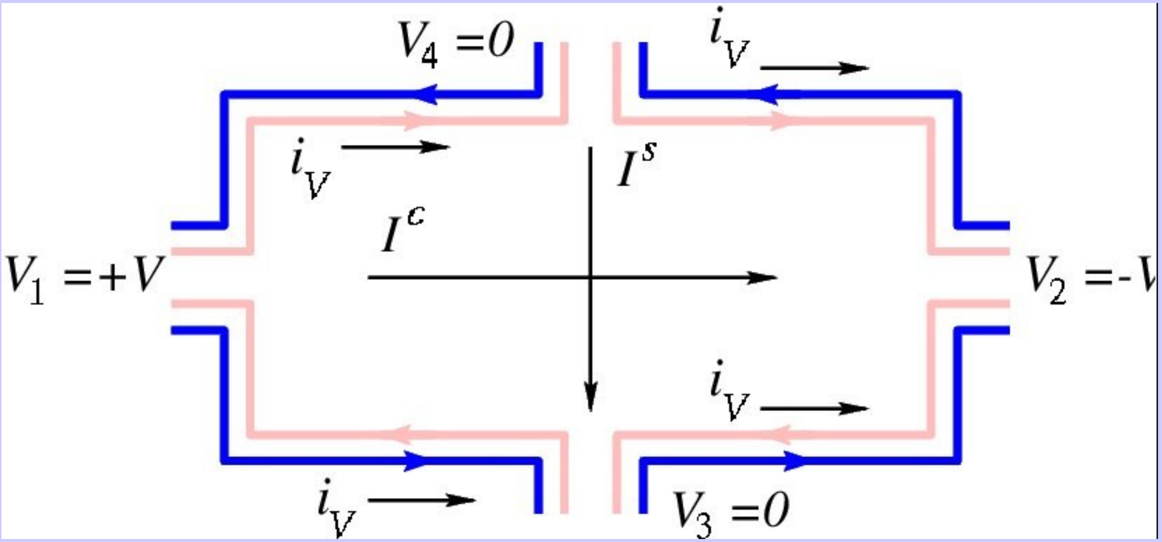

Charge current

$$I_k^c = \sum_{k'} g_{kk'} (V_k - V_{k'})$$

(Landauer-Buttiker)

A 4-terminal device,
full spin mixing in contacts

Spin current $$I_k^s = \sum_{k'} I_{kk'}^s = \sum_{k'} \epsilon_{kk'} g_{kk'} (V_k - V_{k'})$$

where $\epsilon_{kk'} = -\epsilon_{k'k}$ equals $+1$ (-1) when the current from k to k' is carried by spin up (spin down) electrons.

In an ideal clean system (no inter-edge spin-flip scattering):
charge current along V, spin current transverse to V:

$$\rho_{xx} = h/2e^2.$$

Quantized spin Hall conductance

Spin-filtered transport

Asymmetric backscattering filters one spin polarization, creates longitudinal spin current:

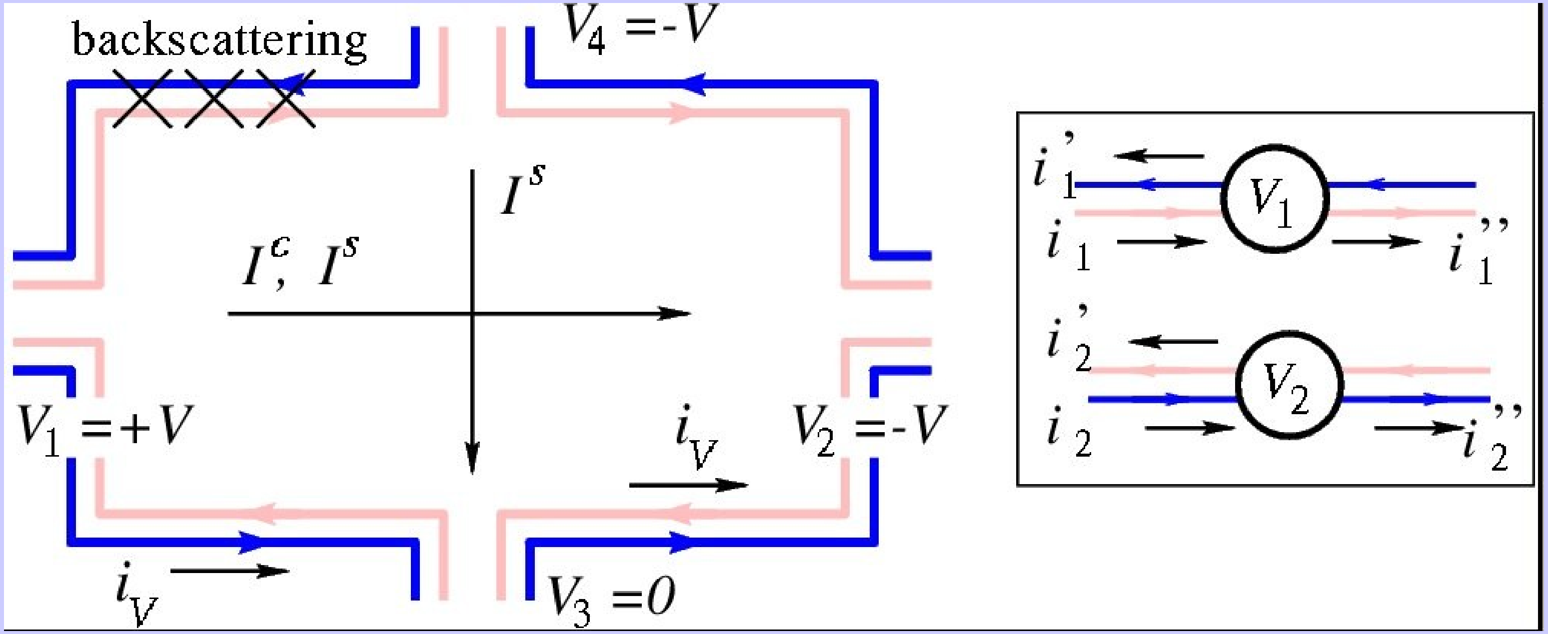

Hall voltage measures spin not charge current!

Applications: (i) spin injection; (ii) spin current detection.

Spin current without ferromagnetic contacts

Control spin-flip scattering?

- Rashba term very small, 0.5 mK;
- Intrinsic spin-orbit substantial, of order 1K, but ineffective when spins are perpendicular to 2d plane;
- In-plane magnetic field tips the spins and allows to tune the spin-flip scattering, induce backscattering
- Magnetic impurities? Oxygen?

Applications for spintronics:

1) Quantized spin Hall effect (charge Hall effect vanishes);

2) Edge transport as spin filter or spin source;

3) Detection of spin current

Estimate of the spin gap

Exchange in spin-degenerate LL's at $\nu=0$, E=0:

- Coulomb interaction favors spin polarization;
- Fully antisymmetric spatial many-electron wavefunction;
- Spin gap dominated by the exchange somewhat reduced by correlation energy:

correlation

$$\Delta = \frac{n}{2}\int \frac{e^2}{\epsilon r}\left(1 - e^{-r^2/2l_B^2}\right) d^2r = \left(\frac{\pi}{2}\right)^{1/2} \frac{e^2}{\epsilon l_B}(1-\alpha)$$

Gives spin gap ~100K much larger than Zeeman energy (10K)

Chiral spin edge states summary

PRL 96, 176803 (2006) and cond-mat/0702125

- Counter-propagating states with opposite spin polarization at $\nu=0$, E=0;
- Large spin gap dominated by Coulomb correlations and exchange
- Experimental evidence for edge transport: dissipative QHE near $\nu=0$
- Gapless edge states at $\nu=0$ present a constraint for theoretical models
- Novel spin transport regimes at the edge

Part III: Strain-induced “magnetic” field:
(i) Aharonov-Bohm effect
(ii) Ordering in Graphene QH Ferromagnet

Nan Gu, Abanin, LL, to be published

Abanin, Lee, LL, cond-mat/0611062, PRL, 2007, to appear

New force in graphene: strain-induced gauge field

Momentum shift due to lattice strain for non-centered valleys: an quasi-B field

Iordanskii and Koshelev, 1985,
Morpurgo and Guinea, 2006,
exp. evidence: Morozov et al, 2005

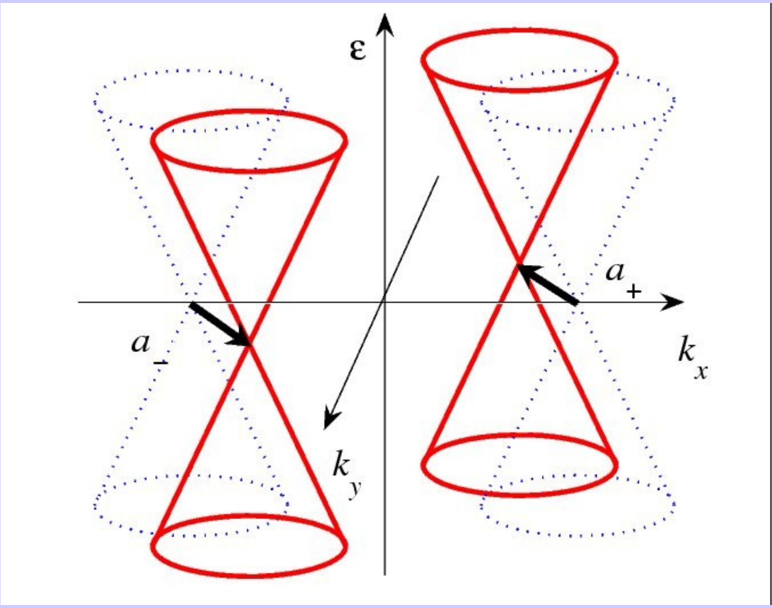

Effective vector potential in the Dirac Hamiltonian:

$$\mathcal{H}_{K,K'} = v(p_i \mp a_i)\sigma_i, \quad a_i = \pm C_i^{jk} u_{jk}, \quad \pm \text{ for } K, K'$$

The trigonal warping tensor

Opposite signs for K and K': time reversal symmetry

Similar to the effect of curvature, twist and shear in Carbon nanotubes (Ando and Kane&Mele)

Microscopic sources of quasi-B field

(i) Microscopic ripples, correlation length ξ

$$\delta h = \nabla \times \mathbf{a}, \quad \langle \delta h_k \delta h_{-k} \rangle \propto k^2, \quad k\xi \ll 1$$

(ii) Dislocations act as solenoids with 1/3 quantum of "quasi-magnetic flux" (geometry only!):

New Aharonov-Bohm effect in graphene:

Katsnelson et al, 2006

a) monochromatic source (Klein tunneling),

b) AB fringes in the diffraction zone (detect with a local probe);

c) macroscopic scale ~10 μm

Magnetic solenoid without coils and batteries

(iii) Acoustic phonons couple to Dirac electrons via magnetic vector potential: nonadiabatic effects outside Born-Oppenheimer apprx, phonon emission by current source

Application to valley-split QHE states

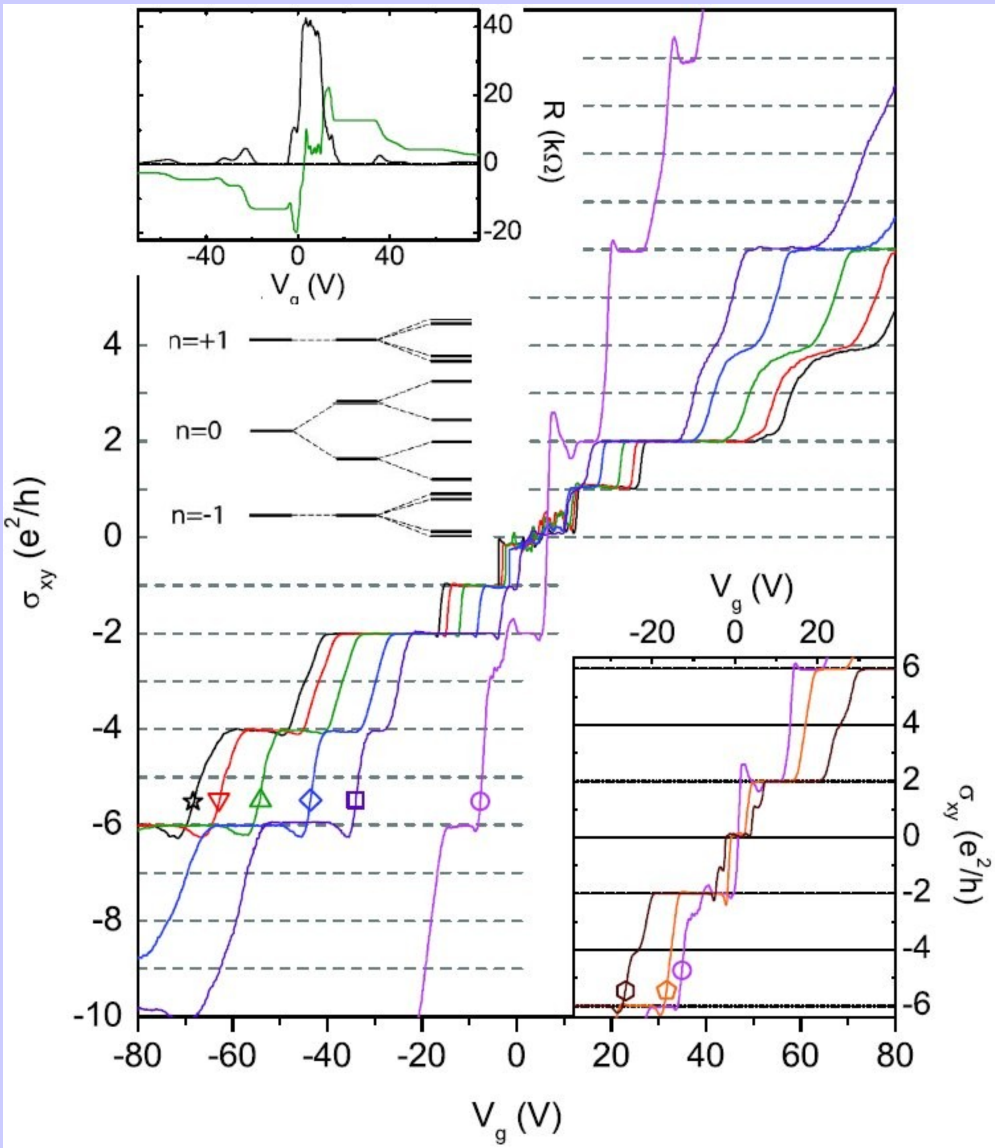

Four-fold degenerate n=0 LL splits into sub-levels at ultra high magnetic field:

spin (n=0,+1,-1), KK' (n=0)

That's what we think ☺

B=9,25,30,37,42,45 Tesla, T=1.4K

(Zhang et al, 2006)

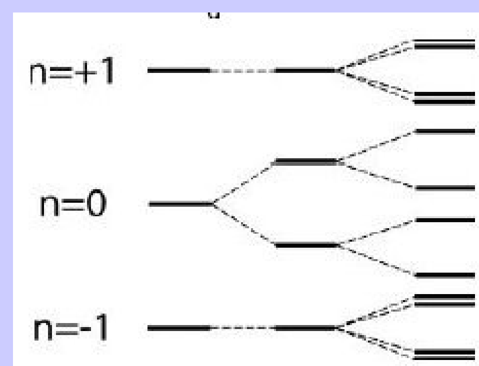

Pseudospin K-K' valley states

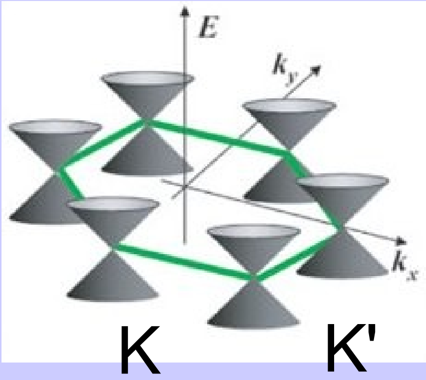

(i) Spin and valley n=0 Landau level degeneracy:

2x2=4;

(ii) SU(4) symmetry, partially lifted by Zeeman interaction:

SU(4) lowered to SU(2), associated with KK' mixing;

(iii) Assume that the ν=1 QHE plateau is described by KK' splitting of spin-polarized n=0 Landau level

Many aspects similar to quantum Hall bi-layers (here KK')
Girvin, MacDonald 1995, and others

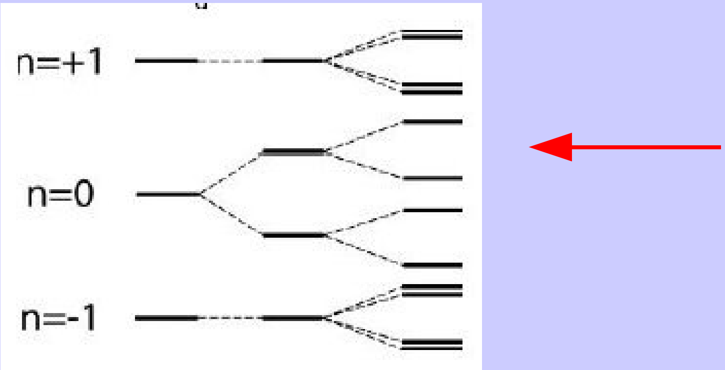

Sigma model for KK'-split LL

The K and K' states at the n=0 LL occupy different sublattices A, B:

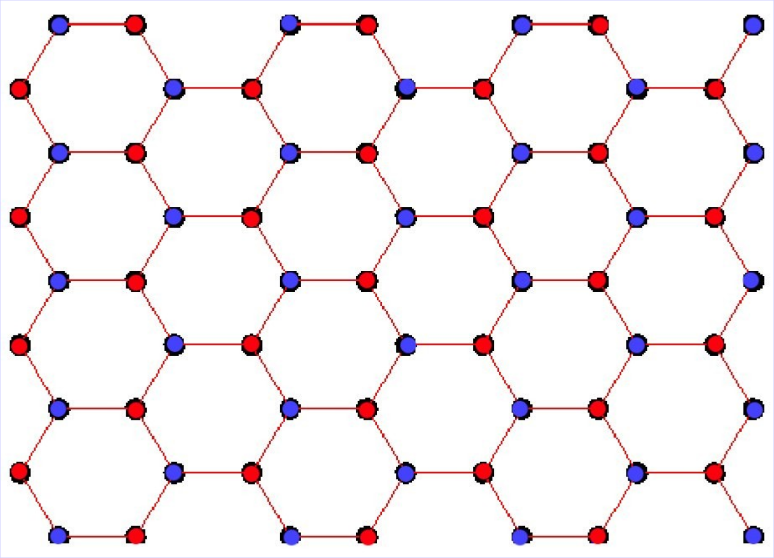

$$\mathcal{H} = \int \left(\tfrac{1}{2} J \nabla \mathbf{n}^2 - \lambda n_3^2\right) d^2x, \quad \mathbf{n} = (n_1, n_2, n_3)$$

Exchange interaction the same as for spin-split LL's;

The anisotropy (Hartree-Fock estimate) is very small:

$$\lambda = l_B^{-4} \left(\sum_{\mathbf{r}\in A} - \sum_{\mathbf{r}\in B} \right) V(\mathbf{r}) \left(1 - e^{-r^2/l_B^2}\right) \approx (a/l_B)^3 e^2/l_B^3 \sim 0.1\,\mathrm{mK}$$

What determines ordering?

Disorder: (i) symmetric (AB or KK') affects energy gap not ordering;

→ (ii) antisymmetric (AB or KK'), couples to vector **n**

→ *Strain-induced B-field provides larger anisotropy*

O(3) sigma model in a random uniaxial "magnetic" z-field

$$\mathcal{H}(\delta h) = g \int \delta h n_3 d^2 x$$

$$\delta h(\mathbf{r}) \parallel \hat{z}$$

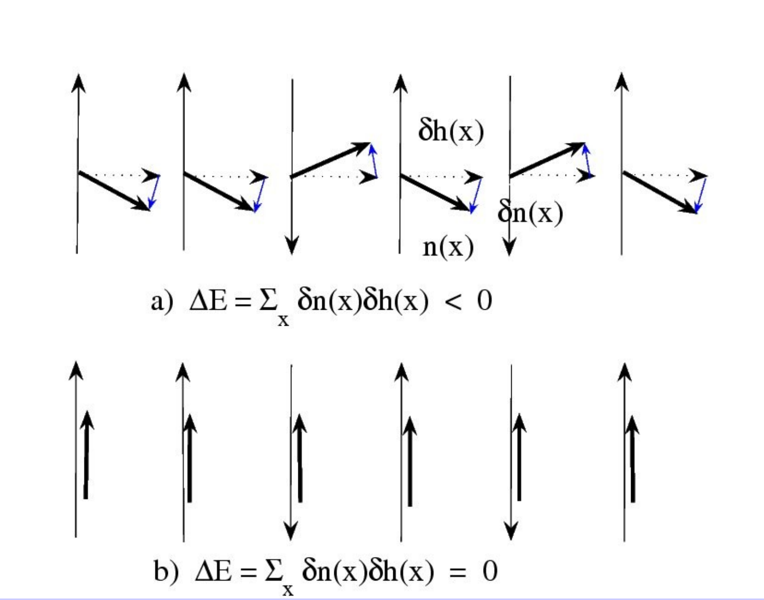

Random field selects an easy plane XY state:

(i) in-plane orientation maximizes energy gain (XY state wins over Larkin-Imry-Ma state);

(ii) analogy with driven inverted pendulum (for Matsubara dynamics use -U instead of U);

(iii) RG averaging over fast fluctuations generates effective easy plane anisotropy;

details in: cond-mat/0611062, PRL, 2007

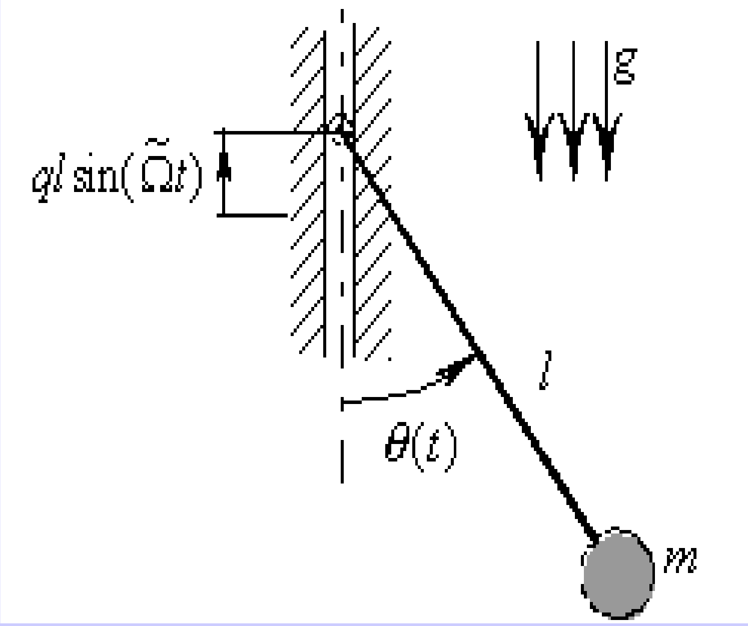

Low energy excitations: fractional skyrmions

- Energy reduced by creating texture, from J to J/2 for a skyrmion of charge e;
- Entropic effects and disorder further suppress the exchange gap;
- Easy plane anisotropy creates XY vortices with e/2 core charge (skyrmions split up as e/2+e/2)

Girvin, MacDonald, 1995

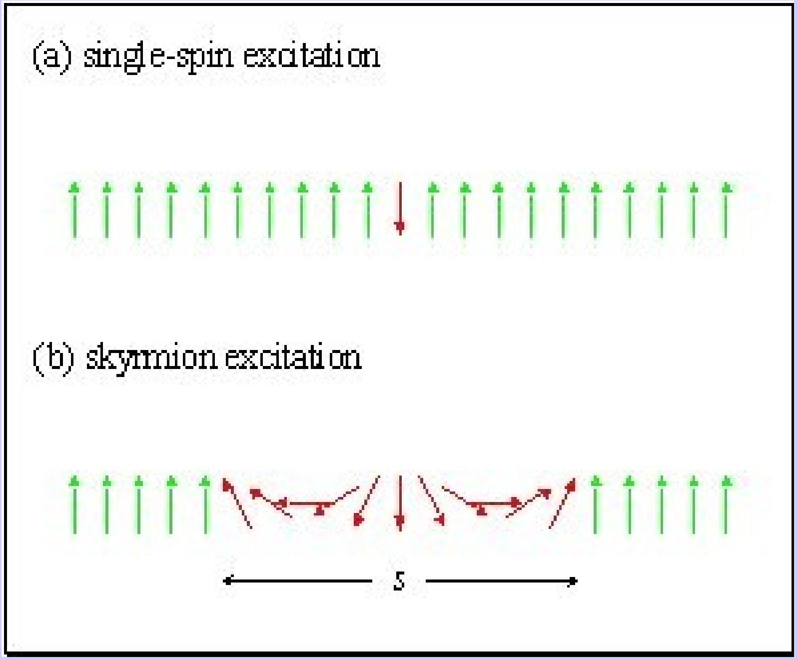

QHE valley splitting summary

- Heisenberg ferromagnet with weak anisotropy;
- Disorder more important than Hartree-Fock anisotropy;
- Random gauge field due to corrugations generates an effective XY anisotropy
- Skyrmions with interesting properties (e/2)

Sigma model for KK'-split LL

The K and K' states at the n=0 LL occupy different sublattices A, B:

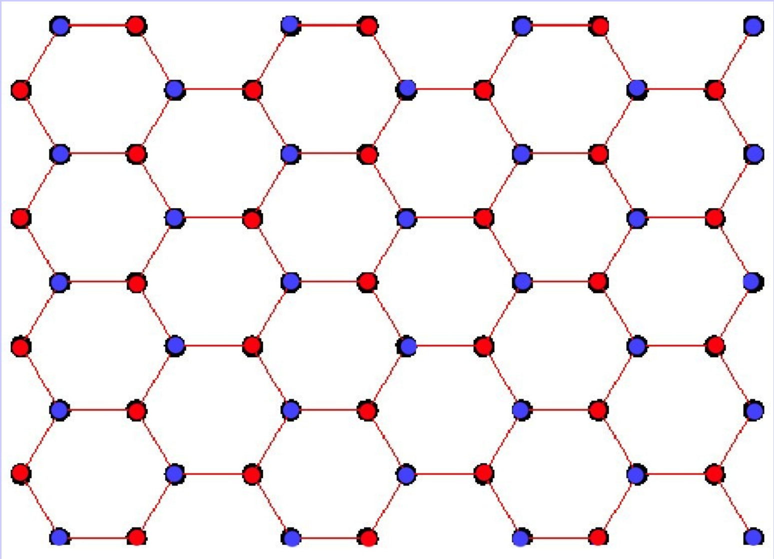

$$\mathcal{H} = \int \left(\tfrac{1}{2} J \nabla \mathbf{n}^2 - \lambda n_3^2\right) d^2x, \quad \mathbf{n} = (n_1, n_2, n_3)$$

Exchange interaction the same as for spin-split LL's;

The anisotropy (Hartree-Fock estimate) is very small:

$$\lambda = l_B^{-4}\left(\sum_{\mathbf{r}\in A} - \sum_{\mathbf{r}\in B}\right) V(\mathbf{r})\left(1 - e^{-r^2/l_B^2}\right) \approx (a/l_B)^3 e^2/l_B^3 \sim 0.1\,\mathrm{mK}$$

What determines ordering?

Disorder: (i) symmetric (AB or KK') affects energy gap not ordering;

→ (ii) antisymmetric (AB or KK'), couples to vector **n**